ACADEMIA ROMÂNĂ
Revue Roumaine de Chimie
https://www.icf.ro/rrch/

Rev. Roum. Chim.,
2026, *71*(3–4), 179–190
DOI: 10.33224/rrch.2026.71.3-4.03

ELECTROCHEMICAL AND ANTIMICROBIAL EVALUATION OF *PISUM SATIVUM* L. PEEL DRY EXTRACT AS A GREEN INHIBITOR FOR *API5L X60* STEEL IN 1 M H_2SO_4

Imen BOUGHAITA,[a,b,*] Nour El Houda SOBHI,[c,d,*] Imane FERAGUENA,[g]
Sihem KHERRAF,[c] Malika FOUDIA[e] and Alain DURAND[f]

[a] Department of Process Engineering, University of 20 Août 1955-Skikda, Skikda, Algeria; i.boughaita@univ-skikda.dz
[b] Laboratory of Chemical Engineering and Environment of Skikda, University of 20 Août 1955-Skikda, Route El-Hadaeik B.P. 26 Skikda, Algeria
[c] Department of Petrochemical, University of 20 Août 1955-Skikda, Skikda, Algeria; kh-sihem@hotmail.fr
[d] Department of Chemistry, Water and Environment Science and Technology Laboratory, Mohamed Cherif Messaadia University, Souk-Ahras, Algeria; n.sobhi@univ-soukahras.dz
[e] Laboratory of Energy and Electrochemistry of Solid (LEES), University Ferhat Abbas Setif 1, Setif, Algeria; foudiam@yahoo.fr
[f] Laboratory of Reactions and Process Engineering (LRGP), UMR 7274, Université de Lorraine – CNRS, Nancy, France; alain.durand@univ-lorraine.fr
[g] Research Laboratory of Interactions, Biodiversity, Ecosystems and Biotechnology, Department of Nature and Life Sciences, Faculty of Sciences, University 20 August 1955, Skikda, 21000, Algeria; i.feraguena@univ-skikda.dz

Received July 5, 2025

There is a growing interest in recycling agricultural waste because more and more people want corrosion protection that lasts. This research examines *Pisum sativum L.* (garden pea) peel extract as an eco-friendly corrosion inhibitor for *API5L X60* steel in 1 M H_2SO_4. Electrochemical methods, such as potentiodynamic polarization (PDP) and electrochemical impedance spectroscopy (EIS), were used to test the extract's antimicrobial activity, inhibition efficiency, and corrosion mechanism. We used scanning electron microscopy (SEM) to look at the surface morphology and Fourier-transform infrared spectroscopy (FTIR) to look at the active functional groups of the inhibitor. Electrochemical and surface analyses demonstrated an inhibition efficiency of up to 78% at a concentration of 0.04 g/L, exhibiting mixed-type inhibition behavior. Adsorption was consistent with the Langmuir isotherm, incorporating both physisorption and chemisorption, and a protective surface layer was noted. The extract also killed a wide range of bacteria, which shows that it could be an eco-friendly, dual-function inhibitor made from agricultural waste.

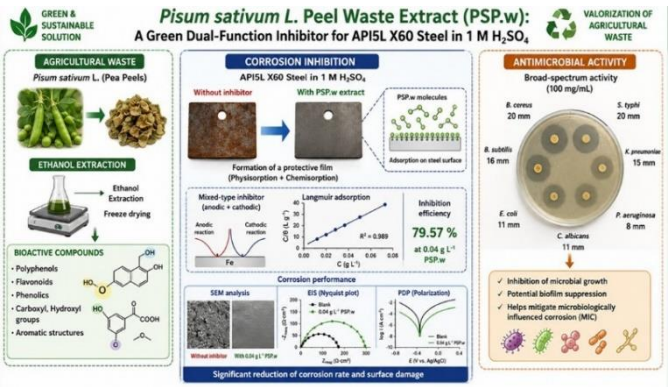

INTRODUCTION

Steel and its alloys are high ductility, toughness, mechanical strength, and malleable industrial materials that are used extensively because of their low cost and ready supply.[1] Nonetheless, its weakness to corrosion in harsh conditions, including HCl and H_2SO_4, is one of the significant

* Corresponding author: n.sobhi@univ-soukahras.dz; https://orcid.org/:0000-0003-0111-2971 (N. E. H. Sobhi); i.boughaita@univ-skikda.dz (I.Bouhaita)

issues brought up by steel.[2] Corrosion normally starts when the metals are exposed to gases, liquids, or water under the influence of air or oxygen. Once the protective barrier is damaged, the corrosion process accelerates; chemical and electrochemical reactions then alter the metal surface and the surrounding environment. Such changes include oxide formation, diffusion of metal cations into coatings, localized pH variations, and changes in electrochemical potential.[1] Examples of economic losses that are caused by metal degradation include the failures of oil pipeline and sewer flooding,[1–3] which is why the development of effective prevention techniques is extremely important. Recently, there have been consistent changes as natural green inhibitors replace traditional ones due to their low cost, ecological benefits, non-toxicity, and the growing demand for safe and sustainable solutions.[4–12] A wide range of plant extracts, such as *castor* oil plant, *citrus peel*, *coconut coir* dust, *aloe vera* gel, *Ginkgo biloba*, *Saussurea obvallata*, *Chamaerops humilis* fruit waste, *Trifolium repens*, gum Arabic, and *Arum dioscoridis*, have been found to have high inhibition efficiencies (up to 70) of steel corrosion in both acidic and neutral environments.[12,15–20] Green corrosion inhibitors prevent metals They are effective primarily because bioactive molecules have polar functional groups that include hydroxyl (–OH), carboxyl (–COOH), amino ($–NH_2$), and thiol (–SH), which are known to adsorb onto metal surfaces to form chemisorbed or physisorbed layers. Also, the aromatic rings and the heteroatoms (N, O, S) are able to contribute electrons or to create complexes with the metal ions, which makes the protective layer more stable. The antioxidants such as flavonoids and other antioxidants neutralize the free radicals, which reduce the electrochemical corrosion, and the alkaloids, tannin, and saponins help in the metal chelation, antioxidant safeguard, and enhanced adsorption. This paper investigates the performance of *Pisum sativum* L. peel waste, a green waste imported from Algeria, as a bioactive compound in inhibiting *API5L X60* steel in H_2SO_4. The inhibitory effect was determined by electrochemical methods, such as potentiodynamic polarization and electrochemical impedance spectroscopy (EIS). The surface morphology was examined with the help of scanning electron microscopy (SEM), and the functional groups involved in the inhibition process were identified using Fourier-transform infrared spectroscopy (FTIR).

Pisum sativum L., commonly known as the garden pea, is a widely cultivated legume that produces a large amount of peel waste during processing and possesses antimicrobial properties as an extract and bioactive agent. This waste contains abundant bioactive compounds, particularly phenolics and flavonoids, which exhibit antioxidant, anti-inflammatory, and antimicrobial activities. Key phytochemicals in pea peel include hesperidin, chlorogenic acid, salicylic acid, apigenin, quercetin, and kaempferol.[23–24] Other compounds such as ascorbic acid, chlorophyll, and proteins enhance the nutritional and functional value of the peel. To the best of our knowledge, this work is the first to use *Pisum sativum* L. peel extract as a corrosion inhibitor for *API5L X60* steel in acidic media, promoting sustainable waste utilization while providing effective corrosion inhibition.

MATERIALS AND METHODS

Extracts preparation

The extraction of *Pisum sativum L*. peel waste (PSP.w) was carried out according to the procedure illustrated in Fig. 1. The peels were first collected, carefully washed, and dried for seven days. The dried peels were then ground into a fine powder and sieved through a 0.5 mm mesh to ensure uniform particle size.

To remove non-polar components, 20 g of the powdered sample was degreased by maceration in n-hexane. The degreased powder was then placed in Erlenmeyer flasks containing an equal volume of ethanol. The mixture was stirred at 200 rpm for 12 hours, after which it was filtered, and the solvent was removed using a rotary evaporator (Rota Vap) at 55 °C. The resulting filtrate was freeze-dried to yield the dried extract (PSP.w). These extracts were subsequently evaluated as natural green corrosion inhibitors in experimental studies.

The concentration of the *Pisum sativum L*. peel extract used as an inhibitor ranged from 0.002 g/L to 0.06 g/L in 100 mL of 1 M H_2SO_4 at room temperature.

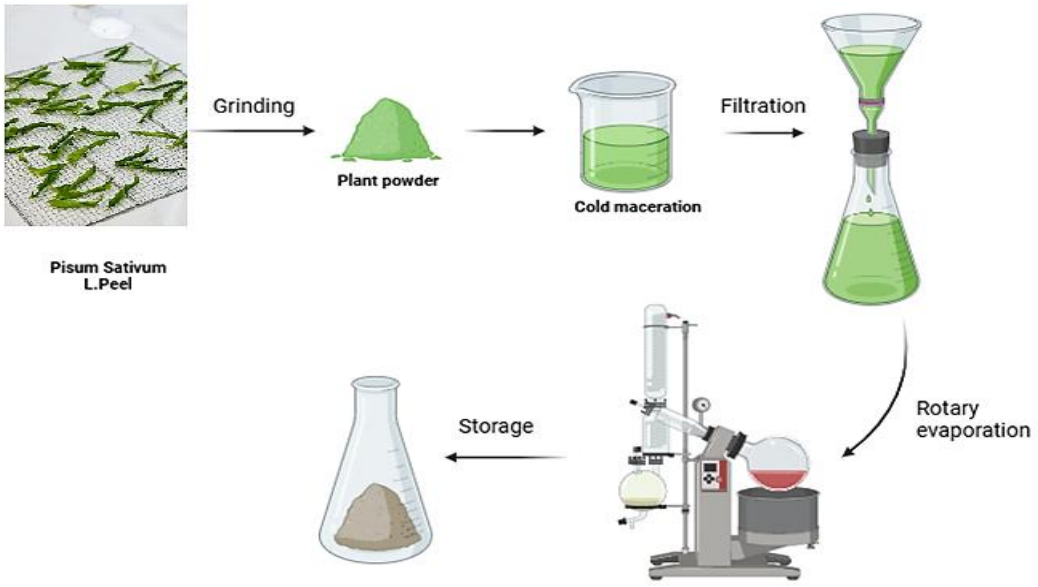

Fig. 1 – Schematic representation of the extraction process of *Pisum sativum L.* peel waste (PSP.w).

Characterization of extracts

The characterization of the extracts (green inhibitors) was performed using Fourier Transform Infrared Spectroscopy (FTIR) with a JASCO FT/IR spectrometer to identify the functional groups. Measurements were conducted in the scanning range of 4000–500 cm^{-1} using the Attenuated Total Reflectance (ATR) technique.

Preparation of electrodes and electrolytes

Steel samples were collected during corrosion inspections at the HBNS (Hassi Berkine North and South – Groupement Berkine) field, located in southern Algeria, west of Hassi Messaoud, within Sonatrach oil operations. The *API5L X60* steel used has a low carbon content and minimal amounts of sulfur and phosphorus. Its relatively high manganese content compensates for the low carbon concentration, improving malleability. The detailed chemical composition of the steel is provided in Table 1.

The working electrode had a surface area of 1 cm^2 and was connected via a copper wire insulated with a thin polystyrene film. Prior to each experiment, the electrode surface was mechanically abraded using a series of emery papers with increasing grit sizes (200, 400, 800, 1000, and 1200). It was then rinsed with distilled water, degreased with acetone, and allowed to dry at room temperature.

Table 1

Chemical composition (wt%) of *API5L X60* steel.

Steel grade	Chemical Composition (%)							
API5L X60	C	Si	Mn	Cr	S	Mo	Ti	Al
	0.06	0.2	1.15	≤ 0.02	≤ 0.025	≤ 0.05	0.03	0.02

All experiments were carried out in a 1 M sulfuric acid (H_2SO_4) solution, prepared from a commercial H_2SO_4 stock solution (96–98% purity) supplied by Honeywell Merck.

Surface examination study

The surfaces of *API5L X60* steel specimens, after exposure to 1 M H_2SO_4 solution in the absence and presence of *Pisum sativum L.* peel waste (PSP.w) at the optimum concentration of 0.04 g/L for 36 h, were characterized by scanning electron microscopy (SEM) using a JEOL JSM-6510LV microscope equipped with an INCA Oxford detector.

Electrochemical measurements

Electrochemical measurements were performed at 300 K using a PGZ301 potentiostat/galvanostat

(Radiometer) coupled with VoltaMaster 4 software. The experiments were carried out in a cylindrical, double-walled glass cell with a capacity of 110 mL, using a three-electrode configuration. The counter electrode was a platinum sheet (1 cm^2), and a saturated Ag/AgCl/KCl electrode was used as the reference. All potentials are reported versus this reference electrode.

The working electrode (*API5L X60* steel) was first immersed in the stagnant solution for 60 min to reach a steady-state open-circuit potential (OCP). After stabilization, potentiodynamic polarization (PDP) curves were recorded at a scan rate of 0.5 mV/s over a potential range of –0.7 V to –0.2 V *vs* Ag/AgCl. Corrosion current densities (I_{corr}) were determined from the Tafel plots by linear extrapolation of the anodic and cathodic branches, and corrosion potentials (E_{corr}) were obtained.

The inhibition efficiency (*IE*, %) and surface coverage (θ) were calculated using the following equations.[28–30]

$$IE(\%)_P = \left(\frac{I_{corr} - I_{corr(inh)}}{I_{corr}}\right) \times 100 \qquad (1)$$

$$\theta = \frac{I_{corr} - I_{corr(inh)}}{I_{corr}} \qquad (2)$$

where I_{corr} and $I_{corr(inh)}$ are uninhibited and inhibited current densities, respectively.

Electrochemical impedance spectroscopy (EIS) measurements were conducted at OCP after 1 h immersion of the steel in the acidic solution. A sinusoidal voltage with an amplitude of 10 mV was applied over a frequency range of 100 kHz to 10 mHz (10 points per decade). Nyquist plots were generated, and the charge-transfer resistance (R_{ct}) values were used to calculate the inhibition efficiency (*IE*, %) as follows:[31]

$$IE(\%)_{(\mathrm{EIS})} \quad \left(\frac{R_{ct} - R_{ct0}}{R_{ct}}\right) \times 100 \qquad (3)$$

where R_{ct0} and R_{ct} are the charge-transfer resistance values without and with (PSP.w) natural, green inhibitors, respectively.

Antimicrobial Activity Assay

The antimicrobial activity of the *Pisum sativum L*. peel ethanolic extract (PSP.w) was evaluated using the agar disc diffusion method. Mueller-Hinton agar was used for bacterial strains, while Sabouraud dextrose agar was employed for the yeast strain, according to standard protocols.[32]

The assay was performed against six bacterial strains: *Bacillus subtilis* ATCC 06024, *Bacillus cereus* ATCC 10876, *Klebsiella pneumoniae* ATCC 700603, *Pseudomonas aeruginosa* ATCC 27853, *Escherichia coli* ATCC 25922, and *Salmonella typhi* ATCC 94028, as well as one yeast strain, *Candida albicans* ATCC 08024.

Microbial suspensions were prepared in sterile saline solution and adjusted to a turbidity equivalent to 0.5 McFarland standard. Sterile filter paper discs were impregnated with 20 µL of the extract dissolved in dimethyl sulfoxide (DMSO) to obtain final concentrations of 100, 50, 25, and 12.5 mg/mL. Discs containing DMSO alone were used as negative controls.

The impregnated discs were placed on the surface of the inoculated agar plates, which were then incubated under appropriate conditions. After incubation, the diameters of the inhibition zones were measured in millimeters. The antimicrobial activity was interpreted based on the inhibition zone diameter criteria described by Ponce *et al*.[33]

RESULTS AND DISCUSSION

FTIR characterization of (PSP.W) extract

The infrared spectrum of *Pisum sativum L*. peel waste (PSP.w) extract is shown in Fig. 2.

FTIR analysis revealed characteristic absorption bands corresponding to various bioactive functional groups. A broad band at 3400–3200 cm^{-1} indicated O-H stretching from phenolic compounds, alcohols, and carboxylic acids, as well as potential N–H stretching from amino acids and proteins. The band around 2900 cm^{-1} suggested C–H stretching of aliphatic hydrocarbons. A prominent peak at 1700 cm^{-1} confirmed C=O stretching from esters, ketones, and aldehydes, while bands in the 1600–1500 cm^{-1} range indicated aromatic C=C stretching (polyphenols) or N–H bending vibrations. The 1400–1200 cm^{-1} region exhibited C–H bending and C–O stretching (esters and phenolic acids), and the peak at 1050 cm^{-1} corresponded to C–O–C/C–O stretching, typical of glycosidic linkages in carbohydrates. The presence of these diverse functional groups highlights the ability of PSP.w to donate electrons and form protective adsorbed layers on metal surfaces, explaining its potential as a corrosion inhibitor.

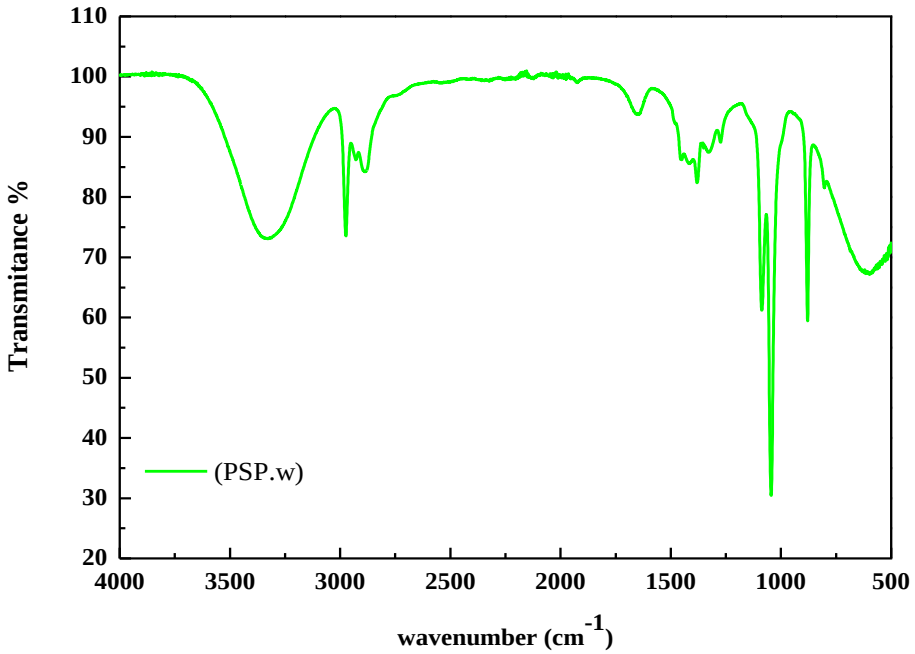

Fig. 2 – FTIR spectrum of PSP.w extract showing main functional groups.

POTENTIODYNAMIC POLARIZATION MEASUREMENTS

Potentiodynamic polarization measurements were conducted to evaluate the inhibitory performance of different concentrations of PSP.w extract in 1 M H_2SO_4 at room temperature. The results for *API5L X60* steel, comparing the absence and presence of varying extract concentrations, are presented in Fig. 3, and the electrochemical parameters derived from the polarization curves are summarized in Table 2. Corrosion parameters were determined by extrapolating the Tafel slopes to the corresponding corrosion potentials. In the absence of the extract, the corrosion potential was measured at –0.500 V *vs* Ag/AgCl. The addition of PSP.w extract, shifted positively the potential to –0.439 V *vs* Ag/AgCl, indicating that the extract influences both anodic and cathodic reactions.

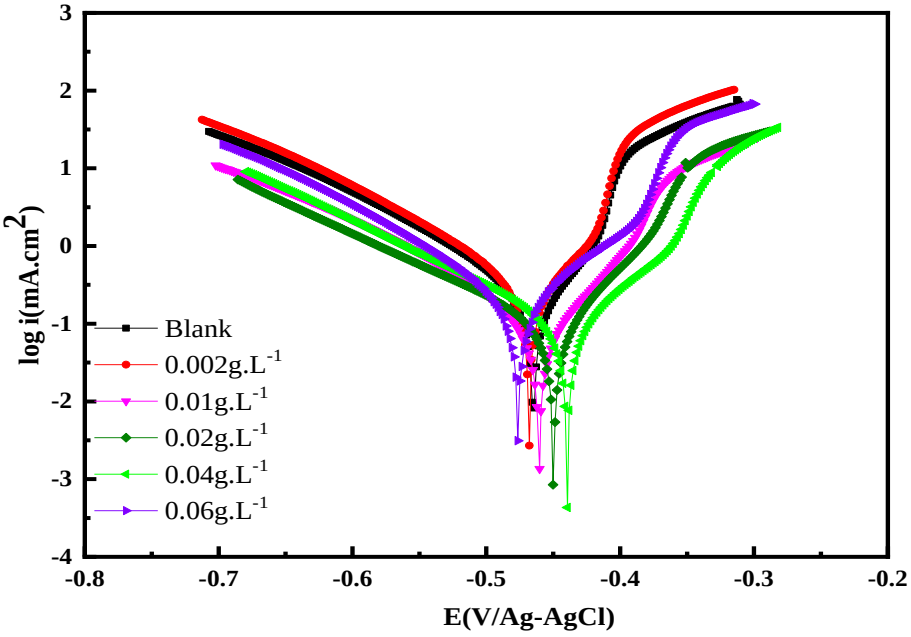

Fig. 3 – Tafel plots of *API5L X60* steel in 1 M H_2SO_4 with and without PSP.w extract.

The increase in polarization resistance (Rp) and the reduction in corrosion current density (I_{corr}), as detailed in Table 2, suggest that PSP.w molecules adsorb onto the steel surface, particularly at active corrosion sites, forming a protective layer. This adsorption enhances the steel's resistance to acid attack, demonstrating the inhibitor's effectiveness even at relatively low concentrations.

Moreover, the reduction in the slopes of the anodic (βa) and cathodic (βc) Tafel lines confirms that PSP.w functions as a mixed-type inhibitor, controlling both anodic metal dissolution and cathodic hydrogen evolution processes [12].

The decrease in inhibition efficiency beyond 0.04 $g \cdot L^{-1}$ suggests that this value corresponds to the optimal inhibitor concentration. The subsequent reduction in inhibition efficiency may be attributed to the saturation of the metal surface by inhibitor molecules, leading to desorption, competitive adsorption, or the formation of less protective multilayer structures that hinder effective surface coverage.

Table 2

Tafel parameters for *API5L X60* steel in 1 M H_2SO_4 with and without PSP.w extract

C (g/L)	E_{corr} (V/Ag-AgCl)	I_{corr} (mA/cm^2)	Rp (Ω.cm^2)	βa(mv/dec)	–βc(mv/dec)	*IE*p%
Blank	–0.465	0.843	26.28	58.7	121.0	/
0.002	–0.468	0.669	33.21	43.3	115.0	**20.62**
0.01	–0.459	0.280	77.89	56.0	111.1	**66.79**
0.02	–0.448	0.206	89.42	63.1	125.7	**75.53**
0.04	–0.439	0.177	95.55	77.0	116.5	**78.92**
0.06	–0.479	0.444	50.35	58.7	103.1	**47.29**

ELECTROCHEMICAL IMPEDANCES SPECTROSCOPY (EIS) MEASUREMENTS

The electrochemical impedance spectra of *API5L X60* steel immersed in 1 M H_2SO_4, in the absence and presence of different concentrations of PSP.w extract, are shown in Fig. 4. These spectra provide a visual representation of the corrosion inhibition performance, highlighting changes in the electrochemical behavior of the steel upon addition of the extract.

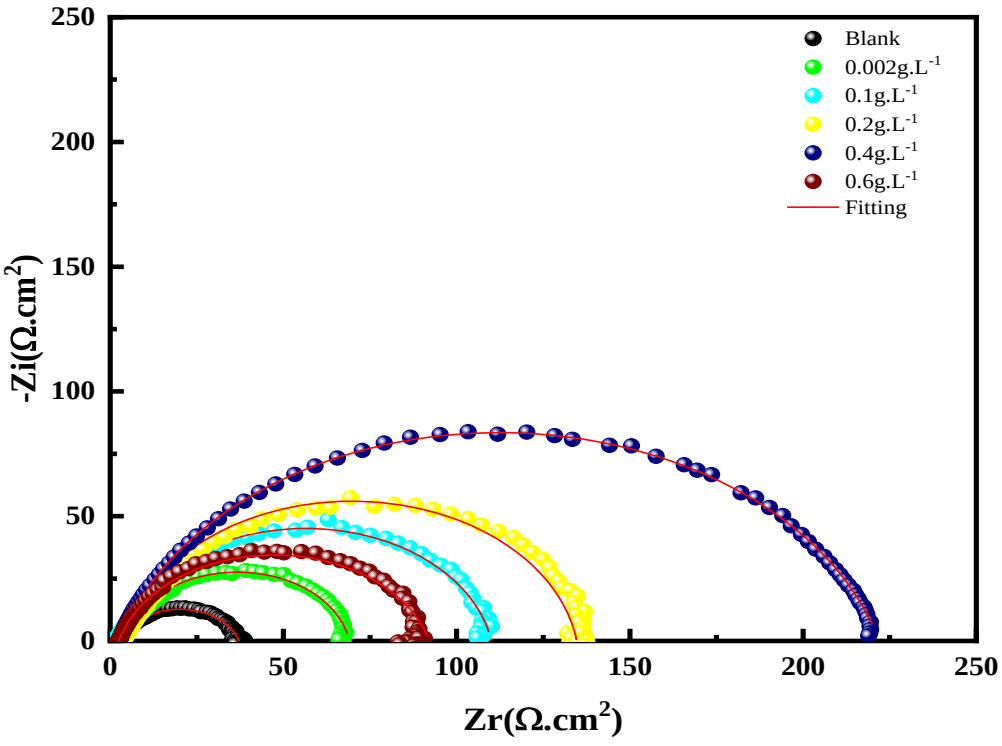

Fig. 4 – Nyquist plots for *API5L X60* steel in 1 M H_2SO_4 with and without PSP.w extract.

The corresponding electrochemical impedance parameters, obtained from fitting the spectra, are summarized in Table 3. Key resistances characterizing the system include the solution resistance (R_s) at the working electrode interface, the charge-transfer resistance (Rct), and the surface film resistance (Rf), which together determine the total polarization resistance (Rp = Rct + Rf).[42–45]

With increasing concentrations of PSP.w extract, the charge-transfer resistance (Rct) and total polarization resistance (Rp) increased significantly, reaching maximum values at 0.04 g/L, which corresponds to the optimal inhibition efficiency of 79.57%. This enhancement is attributed to the formation of a dense and protective adsorbed layer on the steel surface, reducing metal dissolution.

The constant phase elements (CPEs) associated with the electrical double layer also increased with inhibitor concentration, reflecting changes in surface heterogeneity and improved adsorption of PSP.w molecules. The electrical equivalent circuit used to fit the experimental data is depicted in Fig. 5. It consists of the solution resistance (R_s) in series with the parallel combination of polarization resistance (Rp) and a CPE, which replaces the ideal double-layer capacitance (Cdl) to account for non-ideal capacitive behavior. This model provides a reliable representation of the corrosion inhibition mechanism and accurately describes the electrochemical response of the system.

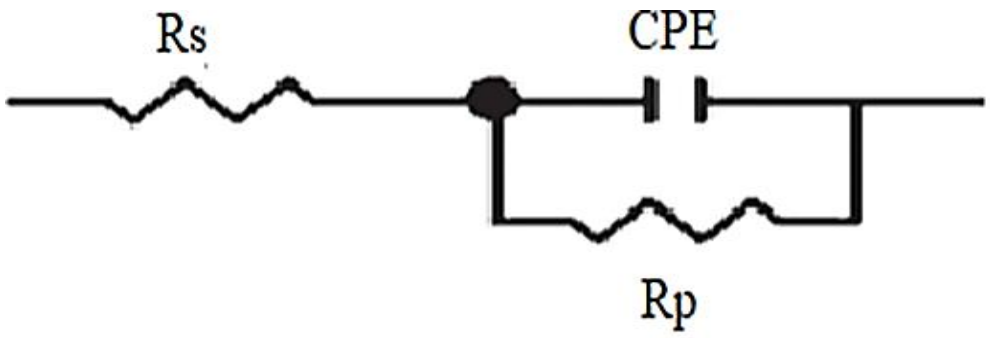

Fig. 5 – Equivalent electrical circuit modeling the metal/solution interface.

Table 3

Electrochemical impedance parameters for API5L X60 steel in 1 M H_2SO_4 with and without PSP.w extract

C (g/L)	Rs ($\Omega \cdot cm^2$)	Rp ($\Omega \cdot cm^2$)	Cdl ($mF \cdot cm^{-2}$)	n	χ^2	IE_{EIS}%
Blank	3.10	42.86	1.151	0.89	0.121	/
0.002	2.40	68.05	0.597	0.88	0.681	**37.02**
0.01	3.39	118.04	0.476	0.89	0.178	**63.69**
0.02	2.97	138.92	0.368	0.88	0.611	**69.15**
0.04	2.27	209.79	0.227	0.82	0.779	**79.57**
0.06	3.62	92.62	0.492	0.83	0.904	**53.72**

SEM MORPHOLOGY SURFACE

The SEM images of *API5L X60* steel surfaces are shown in Figs. 6, 6a shows the surface of the steel specimen before immersion in 1 M H_2SO_4 for 36 hours, revealing a smooth and undamaged surface. In contrast, Fig. 6b illustrates the steel surface after immersion in the acid solution without any inhibitor, showing severe damage, corrosion pits, and roughness due to the aggressive action of H_2SO_4.

Figures 6c and 6d depict the surface morphology of steel treated with 0.04 g/L *Pisum sativum L*. peel waste (PSP.w) extract. These images reveal a smoother surface with a significant reduction in corrosion pits and active sites, indicating the formation of a protective adsorption layer of PSP.w molecules. This protective film effectively mitigates metal degradation and confirms the inhibitor's ability to reduce acid-induced corrosion.

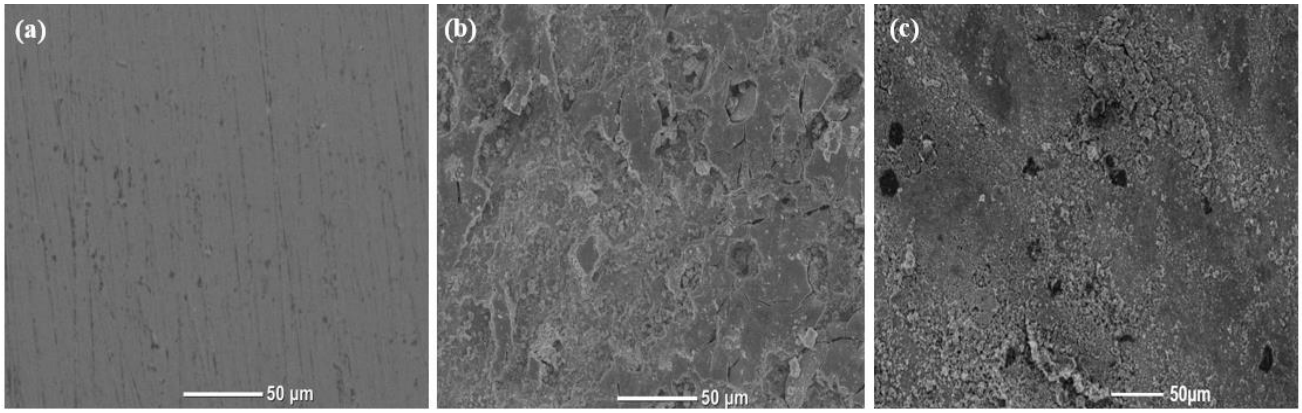

Fig. 6 – SEM micrographs of *API5L X60* steel after 36 h immersion in 1 M H_2SO_4: a) before immersion; b) without inhibitor (blank); c) with 0.04 g/L PSP.w extract.

ADSORPTION ISOTHERMS

Adsorption isotherms are used to analyze how inhibitor molecules interact with metal surfaces by describing the adsorption process, *i.e.*, how organic molecules replace pre-adsorbed water on the metal. Plant-based inhibitors, such as *Pisum sativum L.* peel extract (PSP.w), form protective layers on steel surfaces, blocking active corrosion sites. The adsorption behavior depends on the inhibitor concentration.[37,38]

To investigate the interaction between PSP.w and *API5L X60* steel in 1 M H_2SO_4 at 25 °C, several adsorption isotherm models (Langmuir, Freundlich, and Temkin) were tested. Among these, the Langmuir isotherm provided the best fit, as indicated by the highest correlation coefficient ($R^2 = 0.989$), and can be expressed by the following equation:[39]

$$\frac{C}{\theta} = \left(\frac{1}{K_{ads}}\right) + C \qquad (4)$$

where K_{ads} is the adsorption equilibrium constant, C is the inhibitor concentration, and θ is the surface coverage. Surface coverage values derived from polarization measurements were used to plot the Langmuir isotherm (Fig. 7), confirming its applicability to PSP.w adsorption on steel.[18]

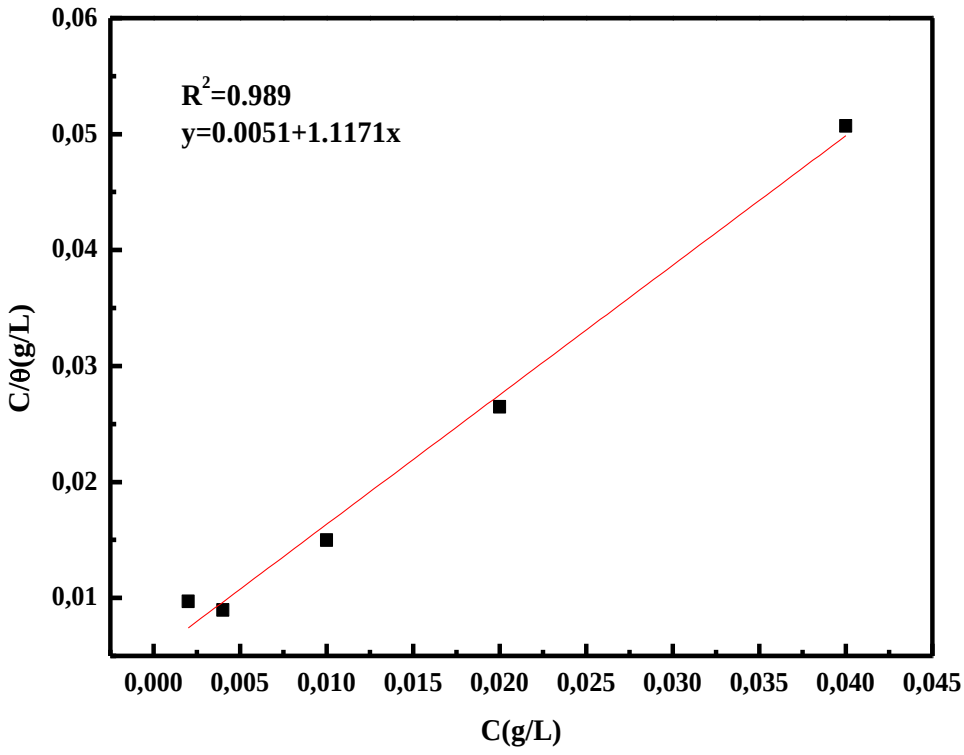

Fig. 7 – Langmuir adsorption isotherm of PSP.w extract on *API5L X60* steel in 1 M H_2SO_4, showing the fit of experimental data.

The Gibbs free energy of adsorption (ΔG°_{ads}) was calculated to evaluate the spontaneity and nature of the adsorption process using the following equation:[39]

$$\Delta G^{\circ}_{ads} = -\mathrm{RT} \ln (K_{ads} \times 1000) \quad (5)$$

where R is the universal gas constant, T is the temperature in Kelvin, and 1000 g/L represents the concentration of water in the acidic medium.

For PSP.w, the calculated ΔG°_{ads} value was –30.214 kJ/mol, which falls within the range of –20 to –40 kJ/mol, indicating that the adsorption mechanism involves both physisorption and chemisorption.[41]

ANTIMICROBIAL ACTIVITY

The antimicrobial activity of the *Pisum sativum* L. peel ethanolic extract is presented in Table 4 and Fig. 8. Antimicrobial activity was mainly observed at the highest tested concentration (100 mg/mL), while little or no inhibition was detected at lower concentrations for most of the tested microorganisms.

The strongest antibacterial activity was recorded against *Bacillus cereus* and *Salmonella typhi*, both showing inhibition zones of 20 mm. Moderate inhibition was observed for *Bacillus subtilis* (16 mm), *Klebsiella pneumoniae* (15 mm), and *Escherichia coli* (11 mm). In contrast, *Pseudomonas aeruginosa* showed the lowest susceptibility, with an inhibition zone of 8 mm.

Residual antibacterial activity was observed for *Bacillus subtilis* at 50 mg/mL (11 mm), whereas no inhibition was detected for most strains at 25 mg/mL and 12.5 mg/mL.

Overall, Gram-positive bacteria appeared slightly more susceptible than Gram-negative bacteria, which may be related to structural differences in their cell walls. The yeast *Candida albicans* exhibited weak antifungal sensitivity (11 mm) at 100 mg/mL.

Table 4

Inhibition zone diameters (mm) produced by the ethanolic extract of *Pisum sativum* L. peel (PSP.w) against bacterial and fungal strains at different concentrations (mg/mL)

Microbial strains	**100 mg/mL**	**50 mg/mL**	**25 mg/mL**	**12,5 mg/mL**
Bacillus subtilis ATCC 06024	16 mm	11 mm	0.9 mm	0 mm
Bacillus cereus ATCC 10876	20 mm	0 mm	0 mm	0 mm
Klebsiella pneumoniae ATCC 700603	15 mm	0 mm	0 mm	0 mm
Pseudomonas aeruginosa ATCC 27853	08 mm	0 mm	0 mm	0 mm
Escherichia coli ATCC 25922	11 mm	0 mm	0 mm	0 mm
Salmonella typhi ATCC 94028	20 mm	0 mm	0 mm	0 mm
Candida albicans ATCC 08024	11 mm	0 mm	0 mm	0 mm

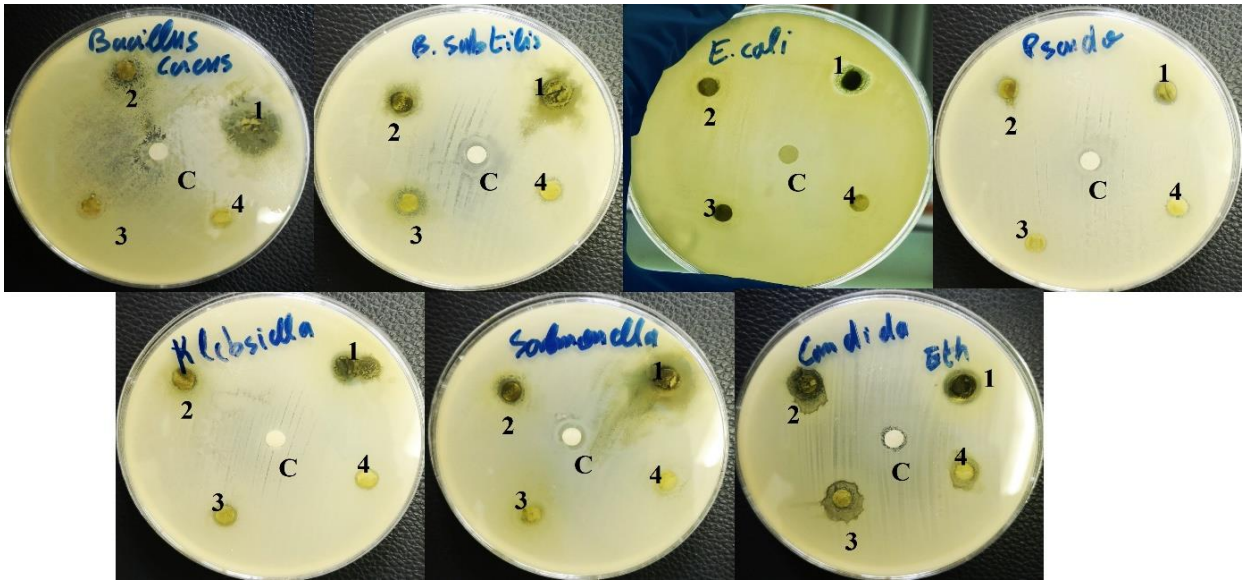

Fig. 8 – Effect of *Pisum sativum L*. peel ethanolic extract (PSP.w) on the tested microbial strains at different concentrations: 1 = 100 mg/mL, 2 = 50 mg/mL, 3 = 25 mg/mL, 4 = 12.5 mg/mL; C = control.

These findings are in agreement with previous studies reporting the antimicrobial potential of *P. sativum* extracts. Hasan *et al.*[44] reported variable antibacterial activity of methanolic seed extracts, with inhibition zones of 11.5 mm for *Pseudomonas* spp., 15 mm for *Citrobacter* spp., and up to 24 mm for *Enterobacter* spp. Similarly, other studies have shown that the antimicrobial efficacy of pea pod extracts strongly depends on the extraction solvent, with ethyl acetate extracts exhibiting the highest activity and minimum inhibitory concentrations ranging from 350 to 850 µg/mL against several bacterial and fungal strains.[45]

The limited antifungal activity observed for this yeast is consistent with previous reports on *Pisum sativum* defensins, which exhibit selective interactions with fungal membrane components rather than broad-spectrum antifungal effects.[46]

The higher susceptibility of Gram-positive bacteria compared to Gram-negative strains may be attributed to differences in cell wall structure, as the outer membrane of Gram-negative bacteria can limit the diffusion of bioactive compounds.[47] The pronounced resistance of *Pseudomonas aeruginosa* is consistent with its known intrinsic resistance mechanisms, including low membrane permeability and active efflux systems.[48]

Although the ethanolic *Pisum sativum* L. peel extract exhibited limited direct antimicrobial activity at the tested concentrations, this effect may still be relevant in reducing microbial biofilm formation, which is a key factor in microbiologically influenced corrosion (MIC).[49] Plant extracts often show modest inhibition of planktonic growth (high MICs), yet can substantially affect biofilm formation and virulence at sub- or near-MIC levels by targeting bacterial signaling, adhesion, or extracellular polymeric substance (EPS) production rather than causing direct microbial killing.[49] Biofilm inhibition without strong growth inhibition has been demonstrated for citrus peel extracts and other plant products through reduced EPS production, altered motility, or disruption of quorum sensing.[50]

Pisum sativum peel extracts are rich in polyphenols and flavonoids and have been reported to exhibit measurable antibacterial activity against both Gram-positive and Gram-negative bacteria, including *Pseudomonas aeruginosa*, with MICs in the mid-hundreds of µg/mL.[45] Ethanolic extracts of *P. sativum* can inhibit *P. aeruginosa* swarming, a biofilm-related behavior, at concentrations above the MIC for growth, supporting a possible biofilm- or virulence-modulating effect.[51]

Because MIC in pipelines is initiated and driven by biofilms at the steel–electrolyte interface,[52,53] even partial suppression of biofilm biomass, EPS production, or microbial motility may reduce pit density and slow localized corrosion, as observed for sulfate-reducing and mixed-consortia biofilms on carbon steels.[52,54] This supports the rationale that a high-dose, weak antimicrobial such as *Pisum sativum* L. peel extract could potentially contribute to biofilm-oriented corrosion mitigation strategies, complementing conventional corrosion inhibitors or biocides.[55,56]

CONCLUSION

The present study demonstrates that *Pisum sativum L.* peel dry extract is an effective green corrosion inhibitor for *API5L X60* steel in 1 M H_2SO_4. FTIR analysis confirmed the presence of bioactive phytochemicals, such as aromatic and phenolic groups, responsible for the adsorption onto the steel surface. Electrochemical measurements (PDP and EIS) and SEM observations indicated that the extract forms a stable protective layer, reducing corrosion rates by up to 79.57% at the optimal concentration of 0.04 g/L. The adsorption process follows the Langmuir isotherm, involving both physisorption and chemisorption, and the extract acts as a mixed-type inhibitor, affecting both anodic and cathodic reactions.

In addition to its anticorrosive properties, the extract exhibits broad-spectrum antimicrobial activity, highlighting its potential to limit biofilm formation and microbiologically influenced corrosion in industrial applications, such as oil and gas pipelines. This work illustrates the feasibility of valorizing agricultural waste as a dual-function green inhibitor, combining environmental sustainability with effective corrosion protection.

Acknowledgements. The authors gratefully acknowledge the support of the Algerian Ministry of Higher Education and Scientific Research (MESRS) and the Directorate General of Scientific Research and Technological Development (DGRSDT) for their assistance and funding.

REFERENCES

1. R. Yıldız, S. Arslanhan, A. Döner, and M. F. Baran, “Materials Chemistry and Physics”, vol. 312, p. 128654, Jan. (2024), doi: 10.1016/j.matchemphys.2023.128654.
2. S. A. Umoren, M. M. Solomon, I. B. Obot, and R. K. Suleiman, *Journal of Industrial and Engineering*

Chemistry, vol. 76, pp. 91–115, (2019), doi: https://doi.org/10.1016/j.jiec.2019.03.057.
3. S. R. Al-Mhyawi, *International Journal of Electrochemical Science*, vol. 18, no. 9, p. 100210, (2023), doi: 10.1016/j.ijoes.2023.100210.
4. H. Wei, B. Heidarshenas, L. Zhou, G. Hussain, Q. Li, and K. (Ken) Ostrikov, *Materials Today Sustainability*, vol. 10, p. 100044, (2020), doi: 10.1016/j.mtsust.2020.100044.
5. S. Z. Salleh *et al.*, *Journal of Cleaner Production*, vol. 304, p. 127030, (2021), doi: https://doi.org/10.1016/j.jclepro.2021.127030.
6. S. Rached *et al.*, *Chemical Data Collections*, vol. 48, p. 101099, (2023), doi: 10.1016/j.cdc.2023.101099.
7. E. Alibakhshi, M. Ramezanzadeh, G. Bahlakeh, B. Ramezanzadeh, M. Mahdavian, and M. Motamedi, *Journal of Molecular Liquids*, vol. 255, pp. 185–198, (2018), doi: 10.1016/j.molliq.2018.01.144.
8. U. J. Timothy, P. S. Umoren, M. M. Solomon, I. O. Igwe, and S. A. Umoren, *International Journal of Biological Macromolecules*, vol. 253, p. 126904, (2023), doi: 10.1016/j.ijbiomac.2023.126904.
9. U. J. Timothy, N. K. Ankah, P. S. Umoren, M. M. Solomon, I. O. Igwe, and S. A. Umoren, *Journal of Environmental Chemical Engineering*, vol. 11, no. 6, p. 111578, (2023), doi: 10.1016/j.jece.2023.111578.
10. M. A. Chowdhury, M. M. S. Ahmed, N. Hossain, M. A. Islam, S. Islam, and M. M. Rana, *Results in Engineering*, vol. 17, p. 100996, (2023), doi: https://doi.org/10.1016/j.rineng.2023.100996.
11. V. Vorobyova, M. Skiba, and E. Gnatko, *South African Journal of Chemical Engineering*, vol. 43, no. 1, pp. 273–295, (2023), doi: 10.1016/j.sajce.2022.11.004.
12. F. Z. Eddahhaoui *et al.*, *Journal of Alloys and Compounds*, p. 173307, (2023), doi: 10.1016/j.jallcom.2023.173307.
13. W. R. De Souza Morais, J. S. Da Silva, N. M. P. Queiroz, C. L. De Paiva E Silva Zanta, A. S. Ribeiro, and J. Tonholo, *Applied Sciences*, vol. 13, no. 13, p. 7482, (2023), doi: 10.3390/app13137482.
14. Z. Zhou, X. Min, S. Wan, J. Liu, B. Liao, and X. Guo, *Results in Engineering*, vol. 17, p. 100971, (2023), doi: 10.1016/j.rineng.2023.100971.
15. C. Liu, Y. Liu, Z. Xia, Z. Wang, and B. Wu, *Journal of Building Engineering*, vol. 82, p. 108194, (2024), doi: 10.1016/j.jobe.2023.108194.
16. X. Sun, Y. Qiang, B. Hou, H. Zhu, and H. Tian, *Journal of Molecular Liquids*, vol. 362, p. 119733, (2022), doi: 10.1016/j.molliq.2022.119733.
17. A. G. Kalkhambkar, S. K. Rajappa, J. Manjanna, and G. H. Malimath, *Inorganic Chemistry Communications*, vol. 143, p. 109799, (2022), doi: 10.1016/j.inoche.2022.109799.
18. S.N. El Houda, B. Amel, & F. Malika, *Journal of the Taiwan Institute of Chemical Engineers*, (2024)165, 105771. doi.org/10.1016/j.jtice.2024.10577.
19. N.H SOBHI, et A. BOUKHOUIETE, *Rev. Roum. Chim*, vol .68. (2023)1-2.02, DOI: 10.33224/rrch.2023.68.1-2.02.
20. A. Döner, R., Yıldız, S., Arslanhan, &M.F.A. Baran., *Journal of the Taiwan Institute of Chemical Engineers*, 169, 105–955. (2025).
21. S. Chen, B. Zhu, and X. Liang, *International Journal of Electrochemical Science*, vol. 15, no. 1, pp. 1–15, (2020), doi: 10.20964/2020.01.39.
22. M. Gabsi *et al.*, *Environ. Sci. Pollut. Res.*, vol. 30, no. 21, pp. 59081–59105, (2023), doi: 10.1007/s11356-023-26753-4.
23. M. Srivastava, P. Tiwari, S. K. Srivastava, A. Kumar, G. Ji, and R. Prakash, *Journal of Molecular Liquids*, vol. 254, pp. 357–368, (2018), doi: 10.1016/j.molliq.2018.01.137.
24. O. D. Ofuyekpone, A. A. Adediran, O. G. Utu, B. O. Onyekpe, and U. G. Unueroh, *J. Electrochem. Sci. Eng.*, (2022), doi: 10.5599/jese.1343.
25. X. Wang, L. Chen, F. Yang, Q. Xiang, and J. Liu, *Journal of Adhesion Science and Technology*, vol. 37, no. 21, pp. 2919–2943, (2023), doi: 10.1080/01694243.2023.2172993.
26. A. Zakeri, E. Bahmani, and A. S. R. Aghdam, *Corrosion Communications*, vol. 5, pp. 25–38, (2022), doi: 10.1016/j.corcom.2022.03.002.
27. R. Haldhar, R. Vanaraj, O. Dagdag, A. Berisha, and S.-C. Kim, *Coatings*, vol. 13, no. 5, p. 860, (2023), doi: 10.3390/coatings13050860.
28. H. G. Ağalar, G. Öztürk, and N. Kırımer, *Eur. J. Life Sci.*, vol. 1, no. 3, pp. 97–106, (2023), doi: 10.55971/EJLS.1148283.
29. I. Meydan, H. Seckin, H. Burhan, T. Gür, B. Tanhaei, and F. Sen, *Environmental Research*, vol. 204, p. 112347, (2022), doi: 10.1016/j.envres.2021.112347.
30. R. S. Abdel Hameed *et al.*, *International Journal of Electrochemical Science*, vol. 17, no. 10, p. 221017, (2022), doi: 10.20964/2022.10.31.
31. B. J. Usman, S. A. Umoren, and Z. M. Gasem, *Journal of Molecular Liquids*, vol. 237, pp. 146–156, (2017), doi: 10.1016/j.molliq.2017.04.064.
32. I. Feraguena, B. Aouzal, F. Boulkenafet, L. Maachia, F. A. Nasr, M. Al-zharani, M. A. Wadaan, and F. A. Al-Mekhlafi, *South African Journal of Botany*, vol. 186, pp. 175–185, (2025), doi: 10.1016/j.sajb.2025.09.013.
33. Ponce, A. G., Fritz, R., Del Valle, C., & Roura, S. I,. *LWT – Food Science and Technology*, 36(7), 679–684, (2003).
34. M. A. EL-Zekred, A. M. Nofal, K. Shalabi, and A. S. Fouda, *Journal of the Indian Chemical Society*, vol. 98, no. 9, p. 100128, (2021), doi: 10.1016/j.jics.2021.100128.
35. A. R. Prasad, K. O. Shamsheera, and A. Joseph, *Journal of the Indian Chemical Society*, vol. 98, no. 4, p. 100052, (2021), doi: 10.1016/j.jics.2021.100052.
36. H. Debab, T. Douadi, D. Daoud, S. Issaadi, and S. Chafaa, *International Journal of Electrochemical Science*, vol. 13, no. 7, pp. 6958–6977, (2018), doi: 10.20964/2018.07.19.
37. A. saxena, D. prasad, and R. haldhar, *Surface Review and Letters*, (2019), doi: 10.1142/S0218625X18502001.
38. H. N. Shubha, T. V. Venkatesha, K. Vathsala, M. K. Pavitra, and M. K. Punith Kumar, *ACS Appl. Mater. Interfaces*, vol. 5, no. 21, pp. 10738–10744, (2013), doi: 10.1021/am4028857.
39. M. A. Amin, *J. Appl. Electrochem.*, vol. 36, no. 2, pp. 215–226, (2006), doi: 10.1007/s10800-005-9055-1.
40. D. Turcio-Ortega, T. Pandiyan, J. Cruz, and E. Garcia-Ochoa, *J. Phys. Chem. C*, vol. 111, no. 27, pp. 9853–9866, (2007), doi: 10.1021/jp0711038.
41. S. Shaban, I. Aiad, M. El-Sukkary, E. Soliman, and M. El-Awady, *Journal of Industrial and Engineering Chemistry*, vol. 21, (2014), doi: 10.1016/j.jiec.2014.05.012.
42. D. Daoud, T. Douadi, H. Hamani, S. Chafaa, and M. Al-Noaimi, *Corrosion Science*, vol. 94, pp. 21–37, (2015), doi: 10.1016/j.corsci.2015.01.025.
43. A. Tazouti *et al.*, *Journal of Molecular Liquids*, vol. 221, pp. 815–832, (2016), doi: 10.1016/j.molliq.2016.03.083.
44. Gonçalves, S., Teixeira, A., Abade, J., de Medeiros, L. N., Kurtenbach, E., & Santos, N. C. , *Biochimica et Biophysica Acta (BBA) – Biomembranes*, 1818(6), 1420–1426. (2012). https://doi.org/10.1016/j.bbamem.2012.02.022

45. Hadrich, F., Elkahoui, S., Gharsallah, N., *et al.*, *Plants*, 12(3), 1–20. (2025), https://doi.org/10.3390/plants 12030674
46. Hasan, R., Hossain, R., Shathi, J. H., Biswas, M. S. *et al*., *KYAU Journal*, 5(2), 58–67. (2022).
47. T. Tavares, J. Antunes, J. Padrão, A. Ribeiro, A. Zille, M. Amorim, F. Ferreira, and H. Felgueiras, *Antibiotics*, vol. 9, (2020), doi: 10.3390/antibiotics9060314.
48. Z. Zhang, *ACS Central Science*, vol. 8, pp. 1043–1046, (2022), doi: 10.1021/acscentsci.2c00750.
49. A. Hamad, *Open Access Journal of Microbiology & Biotechnology*, (2024), doi: 10.23880/oajmb-16000292.
50. P. Dimitrova, V. Ivanova, A. Trendafilova, and T. Paunova-Krasteva, *Pharmaceuticals*, vol. 17, (2024), doi: 10.3390/ph17050573.
51. M. Dazal, E. Gonzales, A. Sabino, R. Salazar, B. Samar, M. Juan, and A. Castillo, *International Journal of Pharmaceutical Sciences and Drug Research*, (2015), doi: 10.25004/ijpsdr.2015.070408.
52. J. Telegdi, J. Telegdi, A. Shaban, and L. Trif, *Microbiologically Influenced Corrosion (MIC)*, pp. 191–214, (2017), doi: 10.1016/b978-0-08-101105-8.00008-5.
53. S. Divi, *Case Studies of Microbiological Influenced Corrosion (MIC) in Pipelines*, CONFERENCE 2025, (2025), doi: 10.5006/c2025-00168.
54. L. Jones, M. Salta, T. Skovhus, K. Thomas, T. Illson, J. Wharton, and J. Webb, *Environmental Microbiology*, vol. 27, (2025), doi: 10.1111/1462-2920.70116.
55. S. Umoren, A. AlAhmary, Z. Gasem, and M. Solomon, *International Journal of Biological Macromolecules*, vol. 117, pp. 1017–1028, (2018), doi: 10.1016/j.ijbiomac. 2018.06.014.
56. A. Alamri, *Engineering Failure Analysis*, vol. 116, p. 104735, (2020), doi: 10.1016/j.engfailanal.2020.104735.